



## RESEARCH ARTICLE

# Altered cerebellar and caudate gray-matter volumes and structural covariance networks preceding dual cognitive and mobility impairments in older people

Pei-Lin Lee<sup>1,2</sup> | Kun-Hsien Chou<sup>2,3</sup> | Wei-Ju Lee<sup>1,4</sup> | Li-Ning Peng<sup>1,5</sup> |  
Liang-Kung Chen<sup>1,5,6</sup> | Ching-Po Lin<sup>2,3,7</sup> | Chih-Kuang Liang<sup>1,8,9</sup>  |  
Chih-Ping Chung<sup>1,10</sup> 

<sup>1</sup>Center for Healthy Longevity and Aging Sciences, National Yang Ming Chiao Tung University, Taipei, Taiwan

<sup>2</sup>Institute of Neuroscience, National Yang Ming Chiao Tung University, Taipei, Taiwan

<sup>3</sup>Brain Research Center, National Yang Ming Chiao Tung University, Taipei, Taiwan

<sup>4</sup>Department of Family Medicine, Taipei Veterans General Hospital Yuanshan Branch, Yi-Lan, Taiwan

<sup>5</sup>Center for Geriatric and Gerontology, Taipei Veterans General Hospital, Taipei, Taiwan

<sup>6</sup>Taipei Municipal Gan-Dau Hospital (managed by Taipei Veterans General Hospital), Taipei, Taiwan

<sup>7</sup>Department of Education and Research, Taipei City Hospital, Taipei, Taiwan

<sup>8</sup>Center for Geriatrics and Gerontology, Kaohsiung Veterans General Hospital, Kaohsiung, Taiwan

<sup>9</sup>Division of Neurology, Department of Internal Medicine, Kaohsiung Veterans General Hospital, Kaohsiung, Taiwan

<sup>10</sup>Department of Neurology, Neurological Institute, Taipei Veterans General Hospital, Taipei, Taiwan

## Correspondence

Dr. Chih-Ping Chung, Center for Healthy Longevity and Aging Sciences, National Yang Ming Chiao Tung University, Taipei Veterans General Hospital, No. 201, Section 2, Shipai Road, Beitou District, 112, Taipei, Taiwan.  
Email: [cpchung@vghtpe.gov.tw](mailto:cpchung@vghtpe.gov.tw)

Dr. Chih-Kuang Liang, Center for Geriatrics and Gerontology, Kaohsiung Veterans General Hospital, No. 386, Dazhong 1st Road, Zuoying District, 813414, Kaohsiung, Taiwan.  
Email: [ck.vghks@gmail.com](mailto:ck.vghks@gmail.com)

## Funding information

Center for Healthy Longevity and Aging Sciences; National Yang Ming University; Center for Geriatrics and Gerontology; Taipei Veterans General Hospital, Taipei, Taiwan; Ministry of Science and Technology, Taiwan, Grant/Award Numbers: NSTC 112-2321-B-075-004, NSTC 112-2321-B-A49-008, 111VACS-001, YSVH11002

## Abstract

**INTRODUCTION:** The neuroanatomical changes driving both cognitive and mobility impairments, an emerging preclinical dementia syndrome, are not fully understood. We examined gray-matter volumes (GMVs) and structural covariance networks (SCNs) abnormalities in community-based older people preceding the conversion to physio-cognitive decline syndrome (PCDS).

**METHODS:** Voxel-wise brain GMV and established SCNs were compared between PCDS and non-PCDS converters.

**RESULTS:** The study included 343 individuals ( $60.2 \pm 6.9$  years, 49.6% men) with intact cognitive and mobility functions. Over an average 5.6-year follow-up, 116 transitioned to PCDS. Identified regions with abnormal GMVs in PCDS converters were over cerebellum and caudate, which served as seeds for SCNs establishment. Significant differences in cerebellum-based (to right frontal pole and left middle frontal gyrus) and caudate-based SCNs (to right caudate putamen, right planum temporale, left precen-tral gyrus, right postcentral gyrus, and left parietal operculum) between converters and nonconverters were observed.

This is an open access article under the terms of the [Creative Commons Attribution-NonCommercial-NoDerivs](https://creativecommons.org/licenses/by-nc-nd/4.0/) License, which permits use and distribution in any medium, provided the original work is properly cited, the use is non-commercial and no modifications or adaptations are made.

© 2024 The Authors. *Alzheimer's & Dementia* published by Wiley Periodicals LLC on behalf of Alzheimer's Association.

**DISCUSSION:** This study reveals early neuroanatomic changes, emphasizing the cerebellum's role, in dual cognitive and mobility impairments.

**KEYWORDS**

caudate, cerebello-frontal network, cerebellum crus II, cerebellum VIII, dual cognitive and mobility decline, gray-matter volume, physio-cognitive decline syndrome, structural covariance, subcortical network, Diagnostic and Statistical Manual of Mental Disorders - III- revised version (DSM-III-R)

**Highlights**

- Neuroanatomic precursors of dual cognitive and mobility impairments are identified.
- Cerebellar GMV reductions and increased right caudate GMV precede the onset of PCDS.
- Altered cerebellum- and caudate-based SCNs drive PCDS transformation.
- This research establishes a foundation for understanding PCDS as a specific dementia syndrome.

## 1 | INTRODUCTION

Physical functions, specifically handgrip strength and gait speed, and cognitive functions are the two critical domains to maintain healthy aging. Both functions naturally decline with age, which is a common aspect of the aging process.<sup>1-3</sup> However, some individuals experience accelerated declines in these functions compared to their age-matched peers. Studies in the literature have increasingly demonstrated that older adults who undergo accelerated deterioration in both physical and cognitive functions face a greater risk of developing dementia compared to those who experience no decline in either domain or who experience decline in only one domain.<sup>3-5</sup> However, little is known about the pathophysiological changes that link the dual cognitive and mobility impairments with future dementia risk.

Physio-cognitive decline syndrome (PCDS) is one of the clinical phenotypes to identify these at-risk community-dwelling older people with combined declines in physical-mobility and cognitive functions.<sup>3,6</sup> It is characterized by simultaneous impairment in mobility without disability (referred to as MIND, which involves slow gait and/or weak handgrip but lacks disabling effects) and cognitive impairment without reaching the level of dementia (referred to as CIND, where cognitive performance falls at least 1.5 standard deviations [SDs] below the mean compared to age-, sex-, and education-matched norms in any cognitive domain yet does not meet the criteria for dementia). Several cohort studies have revealed the prevalence of PCDS in the older community, including 13.3% in Taiwan, 11.2% in Japan, and 18.8% in Singapore.<sup>7-10</sup> These studies also showed that PCDS predicted incident dementia (hazard ratio [HR], 95% confidence interval [CI] = 3.4, 2.4 to 5.0) in older people.<sup>7-10</sup> In a previous neuroimaging

study that cross-sectionally analyzed brain structural changes in older people with PCDS, reductions in regional gray-matter volume (GMV) were observed in the cerebellum, hippocampus, amygdala, thalamus, occipital lobe, and cingulate gyrus.<sup>11</sup> Notably, these regions exhibited certain characteristics distinct from normal aging and neurodegenerative diseases such as Alzheimer's disease (AD).<sup>12</sup> However, they did share similarities with areas showing GMV atrophy in older individuals experiencing mobility frailty, characterized by gait slowness or handgrip weakness.<sup>13</sup> The discovery of distinctive clinical trajectories and brain structural changes in PCDS has ignited hypotheses among our research team and other experts.<sup>3,14,15</sup> The co-occurrence of physical mobility and cognitive decline, or mobility frailty-related cognitive impairment, has raised intriguing possibilities that it might point to a distinct pathophysiological pathway to dementia.

In previous neuroimaging studies, the cross-sectional design constrained our ability to draw definitive conclusions. To address this limitation and validate the observed brain structural changes in older individuals with dual cognitive and mobility impairment PCDS, we sought to explore the temporal relationship between neuroanatomic abnormalities and PCDS. Specifically, we examined the potential of neuroanatomic abnormalities to predict the conversion to PCDS in older individuals. For this purpose, we conducted a longitudinal study comparing voxel-wise GMV and established structural covariance networks (SCNs) in whole-brain MRI scans between individuals who had and had not developed PCDS around 6 years later. The findings of this investigation hold the potential to illuminate early brain mechanisms underlying the simultaneous acceleration of physical mobility and cognitive decline, along with the heightened risk of dementia in older populations.

## 2 | METHODS

### 2.1 | Participants

The study cohort came from the I-Lan Longitudinal Aging Study (ILAS), an ongoing community-based aging cohort that started in 2011. Participants were  $\geq 50$ -year-old community-dwelling adults from Yuanshan Township, I-Lan County. Exclusion criteria included (1) inability to communicate or complete an interview; (2) incapacity to perform simple physical tasks (eg, a 6-min walk test) or cognitive assessments due to poor functional status; (3) presence of any major illness with a life expectancy of less than 6 months; (4) contraindications to magnetic resonance imaging (MRI) such as claustrophobia, ferromagnetic foreign bodies, or metal implants; and (5) a history of neurobiological or neuropsychiatric disorders like stroke, dementia, brain tumor, major depression, or alcohol/substance abuse. The cohort's initial recruitment occurred between January 2011 and July 2014, enlisting a total of 1839 participants.

All ILAS participants underwent anthropometric and physical functional measurements, along with face-to-face neuropsychological assessments administered by trained interviewers. A handgrip strength dynamometer (Smedley's Dynamo Meter; TTM, Tokyo, Japan) was used to measure individuals' muscle strength, which served as a proxy measure of the degree of muscle weakness, and a timed 6-m walk test was used to evaluate participants' walking speed. The neuropsychological tests covered various cognitive domains, including the Mini-Mental State Examination (MMSE), 10-min delayed recall in the Chinese Version Verbal Learning Test (CVVLT), the Boston Naming Test (BNT), the Taylor Complex Figure (TCF) Test, the Backwards Digit Test (BDT), and the Clock Drawing Test (CDT), at each visit. Dementia diagnosis followed the Diagnostic and Statistical Manual of Mental Disorders - III- revised version criteria.

For this study, participants were selected if they were free from dementia and did not meet the criteria for MIND, CIND, or PCDS at baseline (eg, initial sampling wave of ILAS recruited between January 2011 and July 2014) and had received a follow-up during the third wave of ILAS (recruited between September 2018 and January 2021). Brain MRI scans from the baseline assessment were used for analysis.

We conducted this observational cohort study following the Strengthening the Reporting of Observational Studies in Epidemiology (STROBE) guidelines. All participants provided written informed consent after a thorough explanation by research nurses. The study protocol received approval from the Institutional Review Boards of National Yang Ming University (YM103008) and Taipei Veterans General Hospital (2018-05-003B). The study adhered to the principles outlined in the Declaration of Helsinki in terms of its design and execution.

### 2.2 | Definitions of PCDS

All participants within the ILAS cohort (who were free from dementia) were categorized into four distinct subgroups – robust, CIND, MIND,

### RESEARCH IN CONTEXT

- 1. Systematic review:** Recent findings suggest that dual cognitive and mobility decline might represent a distinct pathophysiological pathway to dementia. However, prior neuroimaging investigations into the neuroanatomic underpinnings of this dual decline syndrome have been constrained by small sample sizes and cross-sectional study designs.
- 2. Interpretation:** The study uncovered early regional GMV and morphological network changes preceding PCDS in robust community-dwelling older individuals. PCDS converters exhibited baseline GMV reductions in cerebellum and increased right caudate volumes compared to non-converters. Seed-to-voxel SCN analysis identified distinct covariances in two cerebellum-based and five caudate-based morphological networks (linked to cerebral frontal and temporoparietal regions) between groups. These identified regional GMV and SCN integrity at baseline were also linked to certain physical mobility and cognitive performances over time.
- 3. Future directions:** This research lays a foundation for comprehending PCDS's neuroanatomical basis as a pre-clinical dementia syndrome. Further study may lead to neuroanatomic biosignatures and targeted interventions for those at risk of dual cognitive and mobility impairments. In addition, longitudinal studies across diverse populations can deepen our understanding of these intricate relationships.

and PCDS – using the consensus criteria established by the 2019 Asian Working Group for Sarcopenia. MIND was determined by the presence of gait slowness and/or handgrip weakness, as indicated by the cut-off values defined by the 2019 Asian Working Group for Sarcopenia.<sup>6</sup> Those participants whose cognitive performance fell below 1.5 SDs of the initial sampling study population in any cognitive domain were classified as having CIND. Finally, participants with PCDS were identified as those meeting the criteria for both MIND and CIND.

### 2.3 | MRI data acquisition protocol

All structural MRI data were acquired on a consistent Siemens Tim Trio 3T imaging system (Siemens Medical Solutions, Erlangen, Germany) with a 12-channel head coil at National Yang Ming Chiao Tung University. To obtain tissue volume information and facilitate subsequent seed-to-voxel structural covariance network (SCN) analysis, high-resolution T1-weighted images were acquired using a sagittal three-dimensional T1-weighted magnetization-prepared rapid-acquisition gradient echo sequence (3D-T1w-MPRAGE: repetition time/echo

time/inversion time = 3500/3.5/1100 ms; flip angle = 7°; number of excitations = 1; field of view = 256 × 256 mm<sup>2</sup>; matrix size = 256 × 256; 192 slices, with voxel size = 1.0 × 1.0 × 1.0 mm<sup>3</sup> without any interslice gap and interpolation) for each individual. Prior to further analysis, all raw structural brain images were visually inspected by an experienced neuroradiologist to exclude images affected by movement artifact or notable brain abnormalities, such as trauma, tumors, and hemorrhagic or infarct lesions. Data from 161 individuals did not pass this initial visual quality assessment due to excessive motion and brain abnormalities.

## 2.4 | Structural MRI data processing and quality control

Individual voxel-wise GMV maps were estimated using the voxel-based morphometry analytical framework.<sup>16</sup> This was accomplished by processing the T1-weighted images through the Computational Anatomy Toolbox (CAT12 r1987; <http://www.neuro.uni-jena.de/cat/>) and Statistical Parametric Mapping (SPM12 v7771; <http://www.fil.ion.ucl.ac.uk/spm/>) software within the MATLAB environment (version R2021a; MathWorks, Natick, MA). More specifically, all structural brain images were processed using the CAT12 Diffeomorphic Anatomical Registration Through Exponentiated Lie (DARTEL)<sup>17</sup> pipeline with default settings, incorporating noise reduction, intensity inhomogeneity correction, optimized tissue segmentation,<sup>18</sup> graph-cut skull stripping, and spatial normalization. Of note, customized study-specific tissue templates were used for the DARTEL spatial normalization procedure, and a tissue modulation procedure was also conducted to preserve the actual tissue amount before and after image spatial normalization. Subsequently, all individual modulated gray-matter (GM) images were resampled to the final spatial resolution of 1.5 mm<sup>3</sup> in the standard Montreal Neurological Institute space. In addition, a comprehensive quality control procedure was followed on the raw T1-weighted images and the final preprocessed normalized images. First, the weighted overall image quality rating (IQR) was calculated from the raw T1-weighted images, serving as the first-phase quality control test. Our approach involves utilizing the quality control framework in CAT12, which allows us to evaluate critical image parameters, including noise levels, signal inhomogeneities, and image resolution. These diverse quality metrics were aggregated into a single weighted average IQR quality measure for each individual. This measure was then integrated into a rating scale system that facilitated the comparison of quality measures across different participants. The weighted average IQR values span a range from 100 to 0, where 100 signifies excellent image quality and 0 denotes unacceptable image quality. In this study, we adhered to a criterion, as suggested in prior research, where scans with an IQR value falling below 75% were excluded from our analysis. Second, following the completion of all image preprocessing steps, the covariance structure of all modulated GM images was checked for homogeneity with all other images using the CAT12 “Check Sample Homogeneity” function. The close visual inspection was conducted if

data with covariance were more than two SDs below the mean. Finally, all the verified modulated GMV maps were smoothed with an isotropic Gaussian kernel (full-width half-maximum = 8 mm) and voxels with a GM probability lower than 0.2 were excluded to minimize partial volume effects on different tissue borders. These smoothed, modulated, spatially normalized GM images that passed the quality control procedure were used for the subsequent between-group voxel-wise GMV comparison and seed-to-voxel SCN analysis. For adjusting individual difference in overall brain size, global tissue volume and total intracranial volume (TIV = GM + white matter + CSF volumes) were estimated for each participant in native T1 space using the “Estimate TIV and global tissue volumes” module (part of the CAT12 toolbox).

## 2.5 | Statistical analysis

### 2.5.1 | Demographic and clinical characteristics

All statistical analyses of the demographic and clinical assessments were conducted using IBM SPSS Statistics version 25 (IBM Corp., Armonk, NY, USA). These continuous data were further analyzed using two-sample Student's *t* tests (age and education years) and analysis of covariance analysis (physical mobility and cognitive performance metrics, ANCOVA) to identify statistical differences between the respective study groups and expressed as mean ± SD. The detailed settings of confounding factors were listed in Table 1. A chi-squared test was used to evaluate the differences in proportions of categorical variables (sex, hypertension, diabetes mellitus, dyslipidemia, and smoking status) between groups. A two-sided significance level of *p* values < .05 was considered statistically significant in all analyses.

### 2.5.2 | Multiple comparisons correction and data availability for image-based investigation

SPM12 with appropriate statistical models was used for the following voxel-wise statistical analyses. All reported findings of voxel-wise statistical analyses were corrected for multiple comparisons by means of cluster size correction using command-line tool, which is available in Analysis of Functional Neuroimages software (AFNI, version 22.1.13, <https://afni.nimh.nih.gov/>). More specifically, the updated “3dFWHMx” and “3dClustSim” command-line tools (10,000 Monte Carlo simulations and explicit GM mask) were used to determine a minimum cluster size for maintaining a family-wise error (FWE) rate-corrected *p* value < .05 with an initial cluster-forming voxel-wise threshold of *p* value < .001. Results indicated that clusters larger than 109 voxels were considered significant at a corrected level. All unthresholded voxel-wise statistical maps were uploaded to the NeuroVault repository via the following permanent link (<https://neurovault.org/collections/15130/>) for the purpose of facilitating further visual examination and enabling future image-based meta-analysis.

**TABLE 1** Comparisons of baseline demographics, physical/cognitive function, and global neuroimaging measurements between non-PCDS and PCDS converters.

Demographic variables	Non-PCDS converter (n = 227)	PCDS converter (n = 116)	p value
Age, years, mean ± SD	60.5 ± 6.8	59.5 ± 7.1	.220 <sup>a</sup>
Sex, female, n (%)	129 (56.8%)	44 (37.9%)	.001 <sup>b</sup>
Education, years, mean ± SD	8.7 ± 5.0	9.6 ± 4.3	.086 <sup>a</sup>
Hypertension, n (%)	71 (31.3%)	37 (31.9%)	.907 <sup>b</sup>
Diabetes mellitus, n (%)	22 (9.7%)	16 (13.8%)	.252 <sup>b</sup>
Dyslipidemia, n (%)	9 (4.0%)	6 (5.2%)	.605 <sup>b</sup>
Smoking status, n (%)			.018 <sup>b</sup>
Never	178 (78.4%)	79 (68.1%)	
Current smoker	18 (7.9%)	21 (18.1%)	
Quit smoking	31 (13.7%)	16 (13.8%)	
<b>Physical examination</b>			
Handgrip, kg, mean ± SD	31.1 ± 8.9	34.6 ± 9.0	.808 <sup>c</sup>
Gait speed, m/s, mean ± SD	1.8 ± 0.4	1.8 ± 0.4	.344 <sup>c</sup>
<b>Cognitive performance, scores, mean ± SD</b>			
Mini-Mental State Examination	27.9 ± 2.1	28.2 ± 2.0	.625 <sup>c</sup>
10-min CVLT	7.6 ± 1.2	7.6 ± 1.2	.441 <sup>c</sup>
Clock drawing test	8.9 ± 1.6	9.0 ± 1.4	.281 <sup>c</sup>
Taylor Complex Figure test	33.4 ± 3.6	33.6 ± 3.0	.467 <sup>c</sup>
Boston Naming test	13.5 ± 1.8	13.4 ± 2.2	.034 <sup>c</sup>
Backward Digit test	4.8 ± 1.4	4.7 ± 1.3	.018 <sup>c</sup>
<b>Neuroimaging measurement, cm<sup>3</sup>, mean ± SD</b>			
Total intracranial volume	1354.6 ± 129.2	1386.6 ± 127.3	.684 <sup>d</sup>
Gray-matter volume	592.6 ± 46.8	601.9 ± 46.3	.617 <sup>e</sup>
White-matter volume	483.4 ± 53.8	497.6 ± 53.2	.561 <sup>e</sup>
Cerebrospinal fluid volume	277.2 ± 63.0	285.4 ± 65.2	.859 <sup>e</sup>
WMH volume	1.46 ± 1.71	1.73 ± 2.35	.310 <sup>e</sup>

Abbreviations: CVLT, Chinese version Verbal Learning Test; PCDS, physio-cognitive decline syndrome; WMH, white-matter hyperintensity.

<sup>a</sup>Two-sample t test analysis.

<sup>b</sup>Two-group chi-squared test.

<sup>c</sup>Two-group analysis of covariance adjusted for age, sex and education years.

<sup>d</sup>Two-group analysis of covariance adjusted for age, sex, education years and cigarette smoking status.

<sup>e</sup>Two-group analysis of covariance adjusted for age, sex, education years, cigarette smoking status and total intracranial volume.

### 2.5.3 | Identification of anatomical regions with GMV alterations between non-PCDS converters and PCDS converters

A single-factor two-level ANCOVA model was applied on the individual smoothed GMV images to evaluate GMV difference between two study groups, for example, non-PCDS and PCDS converters. Participants' age, sex, education years, smoking status, and TIV were modeled as covariates of no interest to minimize the potential impact of these variables on the GMV findings. Brain regions surviving the aforementioned statistical criteria were extracted (mean GMV of cluster

and further defined as the candidate seed of interest for subsequent whole-brain seed-to-voxel SCN analyses.

### 2.5.4 | Identification of anatomical regions with structural covariance changes between non-PCDS converters and PCDS converters

To conduct the following seed-to-voxel SCN analyses, two regions-of-interest (ROIs) were first identified from the aforementioned between-group GMV analysis (cerebellum and right caudate). Subsequently, we

used two separate general linear interaction models to explore the potential between-group structural covariance (SC) changes for both cerebellum and caudate ROIs. More specifically, a group main effect term, a mean seed ROI GMV main effect term, and a group  $\times$  mean seed ROI GMV interaction term were contained in a general linear interaction model for each predefined ROI.<sup>19</sup> The same nuisance variables were also included in these constructed models. The between-group difference in the SC strength of the corresponding large-scale SCNs could be identified by assessing the statistical significance of the interaction term at each voxel.

### 2.5.5 | Associations between baseline neuro-morphometrical indices and subsequent physical and cognitive performances

To investigate the potential contribution of identified regional GMV and the integrity of corresponding SC at baseline in subsequent physical mobility and cognitive performances (measured at follow-ups), a series of partial Spearman correlation analyses were conducted. Participants' age, sex, education years, smoking status, and TIV were also included as confounding factors in these correlational analyses. The significance level was set at an uncorrected  $p$  value of  $< .05$  for these exploratory association analyses. Of note, since the aforementioned whole-brain seed-to-voxel SCN analyses were conducted in a group-wise manner, recent research has introduced a diverse array of analytical approaches to quantify the magnitude of SC between two distinct anatomical regions individually, and, notably, the jack-knife bias estimation procedure (leave-one-out approach) has emerged as a widely employed method for characterizing interregional SC integrity and providing subject-level quantitative indices for brain-behavior associational analyses.<sup>20,21</sup> Thus, in this study, we utilized this method to obtain a single measurement to quantify the interregional SC integrities for each individual, which served as inputs for the association analyses.<sup>20,21</sup> First, a reference SC was constructed across all study participants; it was obtained by calculating the partial Pearson correlation coefficient (PCC) between mean GMV of the seed ROI and region with significant SC changes with the seed ROI (identified in the aforementioned between-group seed-to-voxel SCN analyses), with the same nuisance variables being covariates. The reference SC was denoted by  $PCC_n$ . Then we removed participant  $k$  from the study participants and used  $n-1$  subjects ( $n$  indicates the number of study participants) to construct a new SC, which we called the perturbed  $PCC_{n-1}$ . Next, the difference between the perturbed SC and the reference SC was calculated, that is,  $\Delta PCC_n = PCC_n - PCC_{n-1}$ . By subtracting these recalculated SCs from the initial covariance of the full sample, we could estimate the contribution of each participant to the full-sample SC. These calculated values were then normalized to z-scores and referred to as individual SC integrity indices, which were used for further clinical association analysis. The  $\Delta PCC_n$  was converted to the z-score based on the following formula:

$$z = \frac{\Delta PCC_n}{\frac{1 - PCC_n^2}{n-1}}$$

The individual SC integrity for participant  $k$  was then presented with the z-score described by the preceding equation. This individual SC index represents how this participant changed the covariance of pairs of brain regions in their GMV against all study participants.

## 3 | RESULTS

Figures 1, 2, and 3A illustrate the flowcharts of the study designs, participant recruitment data, and neuroimaging analytic process. Initially, we identified 662 participants with preserved cognitive and mobility functions at baseline. Among them, 501 participants met the criteria for qualified brain MRI scans (free from motion artifacts or incidentally found brain lesions). After excluding 150 participants who did not receive a follow-up and eight participants who progressed to dementia during follow-up, the final analysis included baseline brain MRI scans from 343 participants in this study. Participants who received a follow-up were younger and more educated, had less frequent vascular risk factors, and performed better in verbal memory than those who did not receive a follow-up (Table S1). Following an average follow-up period of 5.6 years (SD = 1.0, range = 3 to 8 years), 116 participants had converted to PCDS (Figure 2).

### 3.1 | Comparisons of baseline demographics, physical/cognitive functions, and global neuroimaging manifestations between non-PCDS converters and PCDS converters (Table 1)

Participants who converted to PCDS were more likely to be men and cigarette smokers compared to non-PCDS converters. Both groups exhibited similar performances in physical mobility and cognitive functions, with only slightly poorer scores in BNT and BDT observed in PCDS converters in comparison to non-PCDS converters at baseline. Regarding neuroimaging findings in global brain measurements, PCDS converters and non-PCDS converters showed no significant differences in TIV, GMV, white matter volume, and cerebrospinal fluid volumes at baseline.

### 3.2 | Longitudinal assessment of physical mobility and cognitive functions

Table 2 presents the findings that, on average 6 years later, PCDS converters exhibited significantly slower gait speed and poorer cognitive functions across all domains compared to non-PCDS converters. We also reported the annualized rates of decline in each cognitive and physical domain for both PCDS and non-PCDS converters (Table S2).

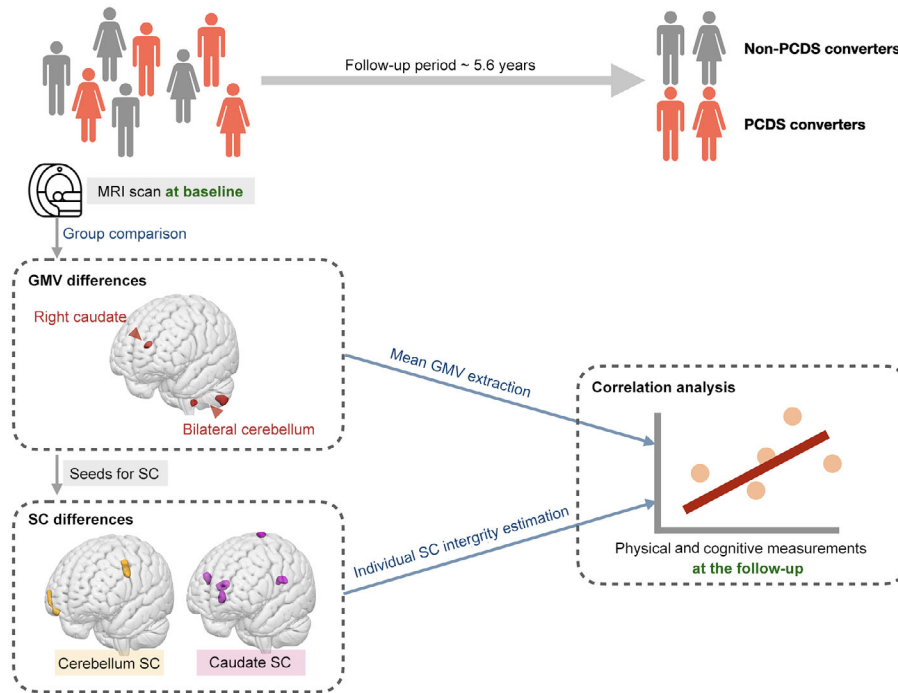


**FIGURE 1** Study design flowchart. The analysis of baseline brain MRI scans from functionally preserved older individuals in the community aimed to detect abnormalities in regional GMV and structural covariance networks (SCNs) preceding the onset of PCDS within a 5.6-year time frame (left). Regions exhibiting abnormal GMV, as revealed by comparisons between PCDS and non-PCDS conversion groups, were used as seed areas to establish SCNs (left). Additionally, group comparisons identified SCNs with abnormal structural covariance in PCDS converters (left). Following this, correlation analyses were utilized to investigate the relationships between these identified neuroanatomical abnormalities and cognitive as well as mobility functions at the follow-up (right). GMV, gray-matter volume; MRI, magnetic resonance imaging; PCDS, physio-cognitive decline syndrome; SCN, structural covariance network.

The results indicated that, despite demonstrating stronger handgrip strength at the follow-up assessment, PCDS converters experienced more rapid declines in all cognitive and physical domains including handgrip strength. Statistical significance was observed in handgrip strength, 10-min CVVLT, CDT, TCF, and the BDT. These results contribute to validating that our PCDS converters indeed experienced dual cognitive and mobility decline.

### 3.3 | Anatomical regions with GMV alterations between non-PCDS converters and PCDS converters

Figure 3A illustrates the neuroimaging analytic framework. The first step, the voxel-based whole-brain analysis, revealed that at baseline, PCDS converters exhibited lower GMV in regions over the right and left cerebellum; however, intriguingly, they displayed higher GMV in the right caudate compared to non-PCDS converters. (Figure 3B and Table 3, family-wise error cluster corrected  $p$  value < .05).

### 3.4 | Cerebellum and caudate-based SC alterations in PCDS converters

For the second step, the seed-to-voxel SCN analyses (Figure 3A), we utilized the regions in the cerebellum and caudate that exhibited

altered GMV in PCDS converters as ROIs. Subsequently, successful establishment of the SCNs for these two regions was achieved. At baseline, two cerebellum-based and five caudate-based structural networks showed significantly different SCs between non-PCDS and PCDS converters (Figure 3C and Table 3).

Specifically, around 6 years prior to the conversion to PCDS, the cerebellum displayed decreased morphological covariances with the right frontal pole and left middle frontal gyrus in PCDS converters. Among the five identified altered caudate-based structural networks, PCDS converters demonstrated decreased morphological covariances between caudate and another region in the caudate and putamen. Simultaneously, they exhibited increased morphological covariances between caudate and right planum temporale, left precentral gyrus, right postcentral gyrus, and left parietal operculum cortex at baseline when compared with non-PCDS converters.

### 3.5 | Correlations between each identified regional GMV or related SCN's integrity and subsequent physical mobility/cognitive functions (Figure 4, Table S3)

The primary aim of our study was to identify the early neuroanatomic pathophysiology associated with accelerated cognitive and mobility declines in community-based older individuals, specifically comparing

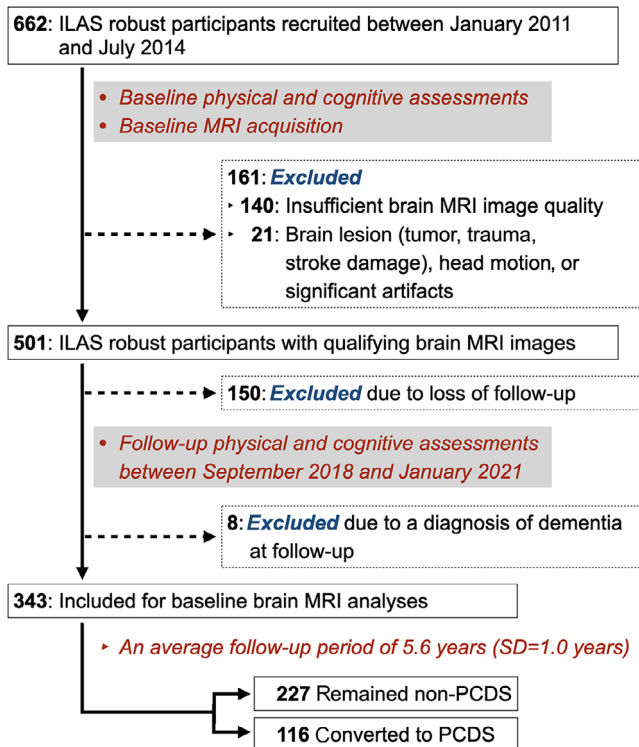


**FIGURE 2** Study population recruitment. Participants meeting the following criteria were included in the study: absence of dementia, no indication of mobility impairment, cognitive impairment, or PCDS during initial sampling wave of ILAS, which occurred between January 2011 and July 2014. These participants underwent follow-up during the third wave of ILAS, conducted between September 2018 and January 2021. Excluded individuals comprised those with MRI scans of inadequate quality, significant brain lesions, loss of follow-up, or a diagnosis of dementia during the follow-up assessment. After an average follow-up period of 5.6 years ( $SD = 1.0$ , range = 3–8 years), a total of 116 participants had converted to PCDS. ILAS, the I-Lan Longitudinal Aging Study; MRI, magnetic resonance imaging; PCDS, physio-cognitive decline syndrome; SD, standard deviation.

non-PCDS and PCDS converters through group-level analyses. In an effort to validate the identified neuroanatomic correlates of PCDS, we extended our investigation to explore the connections between these abnormalities and subsequent cognitive and mobility functions at an individual level, which was the third step of our neuroimaging framework (Figures 3A and 4).

The results showed that the baseline regional GMVs in the cerebellum displayed significant positive correlations with visuospatial function (TCF test) and handgrip strength at the follow-up assessment. However, the integrity of cerebellum-based SCNs at baseline showed no associations with subsequent physical mobility and cognitive performances (Figure 4, Table S3).

Conversely, the baseline regional GMV in the caudate did not exhibit associations with any subsequent physical mobility and cognitive performances. However, the integrity of caudate-based SCNs at baseline displayed significant associations with several physical mobility and cognitive functions at follow-ups. Specifically, the integrity of SCN

between caudate and caudate/putamen showed positive associations with handgrip strength and gait speed, while those of SCNs between caudate and right planum temporale, left precentral gyrus, and right postcentral gyrus were negatively associated with visuospatial executive (CDT), language (BNT), and executive (BDT) functions, respectively (Figure 4, Table S3).

Notably, the significance level was set at an uncorrected  $p$  value of  $< .05$  for these exploratory association analyses. The detailed results of Spearman correlation analysis are provided in Table S3.

## 4 | DISCUSSION

This study revealed early regional GMV and morphological network changes preceding PCDS in community-dwelling older individuals. PCDS converters exhibited baseline GMV reductions in cerebellum and increases right caudate volumes compared to nonconverters. Seed-to-voxel SCN analysis identified distinct covariances in two cerebellum-based and five caudate-based morphological networks (linked to cerebral frontal and temporoparietal regions) between groups. These findings offer an understanding of the neuroanatomical foundation of rapid declines in both physical mobility and cognitive functions, potentially guiding targeted prevention of subsequent dementia in those older people with dual cognitive and mobility impairments.

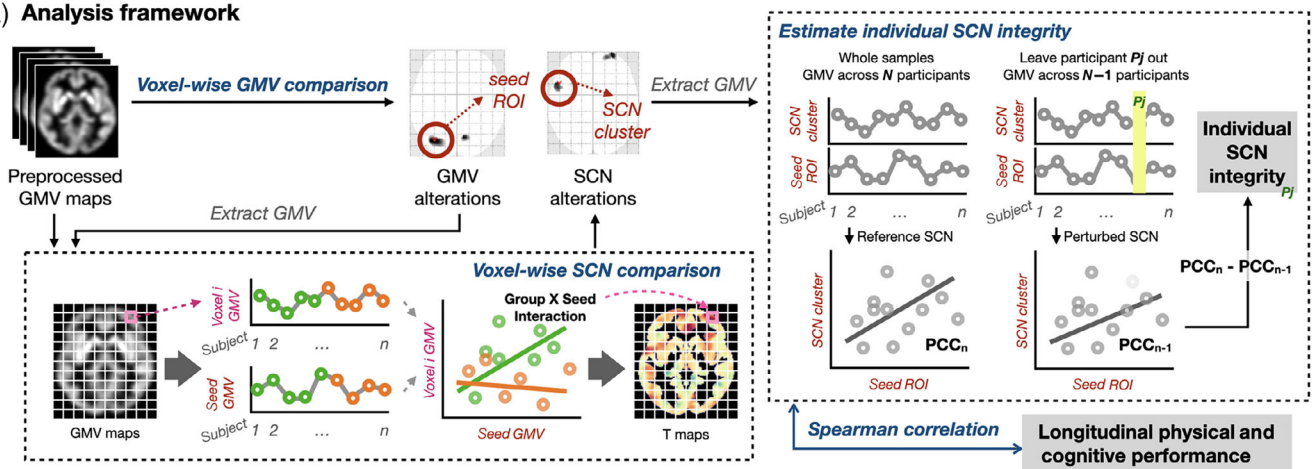
Recent advancements in understanding the cerebellum, initially recognized for motor coordination, have revealed its multifaceted role in cognitive, emotional, and behavioral functions, as well as its impact on age-related disorders.<sup>22,23</sup> This study identifies specific cerebellar regions – left crus II (part of VIIa) and right VIIIa – associated with the conversion to PCDS. Notably, recent neuroimaging studies emphasize the involvement of cerebellar crus I/II and VIII regions in various brain networks supporting cognitive functions such as working memory, episodic memory, navigation, and attention.<sup>24–27</sup> Our findings further emphasize the role of cerebellar crus II and VIIIa in the accelerated decline of mobility and cognitive function in older individuals.

### 4.1 | Cerebellum in mobility frailty and related cognitive impairment

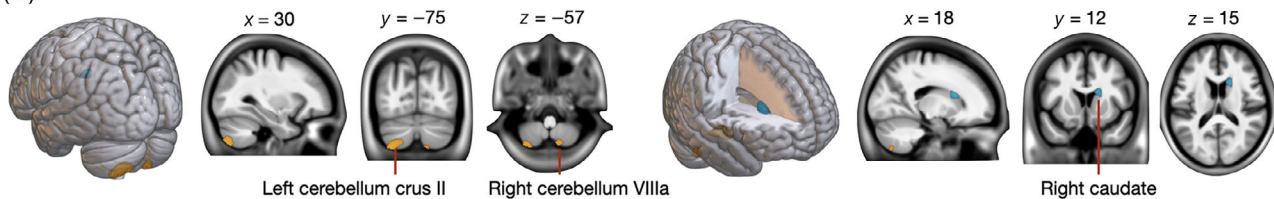
Physical frailty, an accelerated decline in physical function seen in older individuals, evaluates five indicators: weight loss, exhaustion, handgrip weakness, physical inactivity, and slow gait speed.<sup>28</sup> Research, including ours, demonstrates that physical frailty, especially with gait slowness, links to cognitive impairments beyond memory function and raise dementia risk in older adults.<sup>15,29,30</sup> Our prior research first unveiled neuroanatomic links to each physical frailty component, identifying reduced cerebellum GMV notably linked to gait slowness, handgrip weakness, and physical inactivity.<sup>13</sup> Notably, these elements, termed mobility frailty, exhibit stronger correlations with cognitive impairments among the five frailty components.<sup>3,7–9,14,15,30</sup>



## (A) Analysis framework



## (B) GMV alterations in PCDS converter



## (C) SCN alterations in PCDS converter

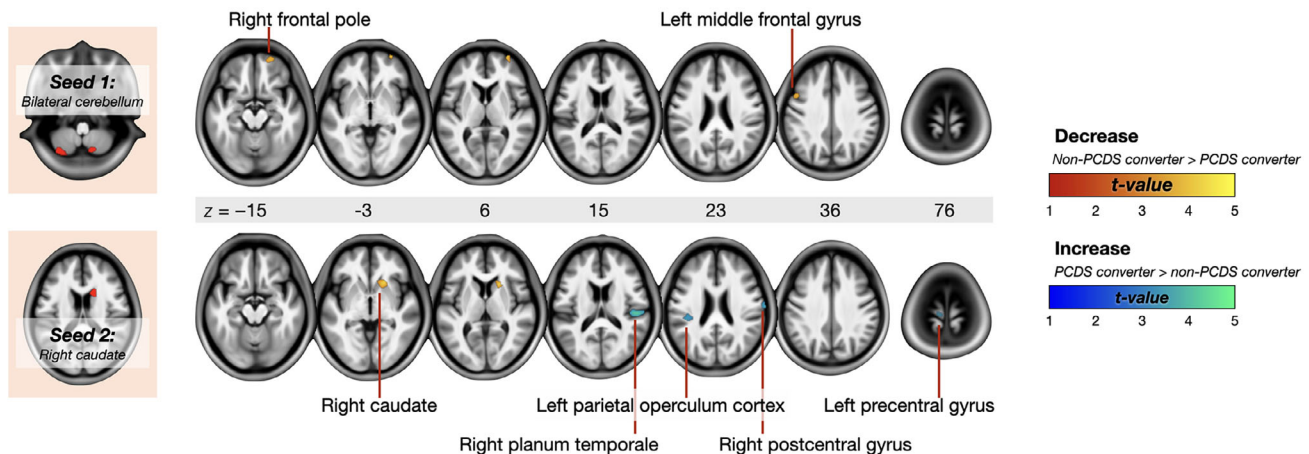


**FIGURE 3** Study analytic framework (A) and alterations in regional GMV (B) and SCNs (C) found in PCDS converters. (A) The analysis of baseline brain MRI scans from community-dwelling older individuals aimed to identify anomalies in regional GMV and SCNs preceding the onset of PCDS over a 5.6-year duration. Regions displaying abnormal GMV, identified through comparisons between PCDS and non-PCDS conversion groups, served as seed areas to construct SCNs. Group comparisons were conducted to pinpoint SCNs exhibiting abnormal structural covariance specifically in PCDS converters. Finally, correlation analyses were employed to explore the connections between these identified neuroanatomical irregularities and subsequent cognitive and mobility functions during the follow-up period. (B) Our neuroimaging framework first involved voxel-wise GMV comparisons, revealing lower GMV in the cerebellum and higher GMV in the right caudate in PCDS converters at baseline. (C) In the subsequent step, seed-to-voxel SCN analyses utilized cerebellum and caudate regions with altered GMV as ROIs. We established SCNs for these regions, with two cerebellum-based and five caudate-based networks showing significant differences between non-PCDS and PCDS converters at baseline. GMV, gray-matter volume; PCC, Pearson correlation coefficient; PCDS, physio-cognitive decline syndrome; ROI, region of interest; SCN, structural covariance network.

A recent extensive study using the UK Biobank dataset also found cerebellum and other brain regions with significantly reduced GMV in people with physical frailty.<sup>31</sup> In their study, cerebellum, accumbens, thalamus, hippocampus, brain stem, anterior temporal fusiform cortex, parahippocampus, temporal pole, and pallidum showed pro-

nounced associations with physical frailty. Intriguingly, they indicated that reduced GMV in these regions significantly mediated the link between physical frailty and cognitive impairments.

These findings, highlighting unique cognitive and neuroanatomic traits in physical mobility frailty, lead us and fellow researchers to

**TABLE 2** Comparisons of longitudinal physical/cognitive function between non-PCDS and PCDS converters.

Demographic variables	Non-PCDS converter (n = 227)	PCDS converter (n = 116)	p value <sup>a</sup>
<b>Physical examination</b>			
Handgrip, kg, mean ± SD	32.3 ± 9.2	33.8 ± 10.4	.002
Gait speed, m/s, mean ± SD	1.0 ± 0.3	0.9 ± 0.2	<.001
<b>Cognitive performance, scores, mean ± SD</b>			
Mini-Mental State Examination	28.1 ± 2.2	28.1 ± 2.4	.142
10-min CVVLT	7.8 ± 1.7	6.9 ± 2.2	<.001
Clock drawing test	9.0 ± 1.5	8.4 ± 2.2	<.001
Taylor complex figure test	29.0 ± 5.5	25.9 ± 6.0	<.001
Boston naming test	12.6 ± 2.2	12.2 ± 2.8	.005
Backward digit test	4.8 ± 1.7	4.3 ± 1.9	<.001

Abbreviations: CVVLT, Chinese version Verbal Learning Test; PCDS, physio-cognitive decline syndrome.

<sup>a</sup>Two-group analysis of covariance adjusted for age, sex, and education years.

**TABLE 3** Anatomical regions with significant altered gray-matter volume and structural covariance in non-PCDS and PCDS converters.

Maximum t-value	Cluster size	MNI coordinate (x, y, z)	Anatomical region
<u>Gray-matter volume</u>			
<b>Non-PCDS converter &gt; PCDS converter</b>			
3.63	588	-31, -77, -55	Left cerebellum crus II
3.56	150	12, -71, -59	Right cerebellum VIIIa
<b>Non-PCDS converter &lt; PCDS converter</b>			
3.75	189	15, 17, 20	Right caudate
<u>Structural covariance (seed: bilateral cerebellum)</u>			
<b>Non-PCDS converter &gt; PCDS converter</b>			
4.12	358	30, 66, -2	Right frontal pole
3.96	342	-51, 17, 47	Left middle frontal gyrus
<u>Structural covariance (seed: right caudate)</u>			
<b>Non-PCDS converter &gt; PCDS converter</b>			
4.51	436	20, 20, 0	Right caudate/putamen
<b>Non-PCDS converter &lt; PCDS converter</b>			
4.26	466	53, -23, 14	Right planum temporale
3.93	144	-11, -21, 81	Left precentral gyrus
3.74	152	69, -11, 27	Right postcentral gyrus
3.41	153	-41, -29, 24	Left parietal operculum cortex

Abbreviation: PCDS, physio-cognitive decline syndrome.

propose that mobility frailty-related cognitive declines and ensuing dementia might denote an unexplored, novel neurodegenerative disorder. To investigate its underlying mechanisms, researchers have introduced operational definitions such as the PCDS, the Motoric Cognitive Risk (MCR) syndrome and the dual decliner (refers to individuals who exhibit decline in both memory and gait over a longitudinal period).<sup>3,14,15</sup> These definitions outline the co-occurrence of physical mobility and cognitive declines, utilizing diverse criteria for characterization.

## 4.2 | Cross-sectional neuroimaging studies

Cross-sectional neuroimaging research on MCR syndrome, characterized by slow gait and cognitive complaints without dementia, has linked it to reduced GMV and altered SCN in prefrontal cortex, supplementary motor area, and insula. However, these studies had limited sample sizes (28 to 38 MCR cases) and usually overlooked the cerebellum.<sup>32,33</sup> In contrast, our prior cross-sectional study (190 PCDS cases) using voxel-wised whole-brain analyses revealed lower GMV in amygdala,

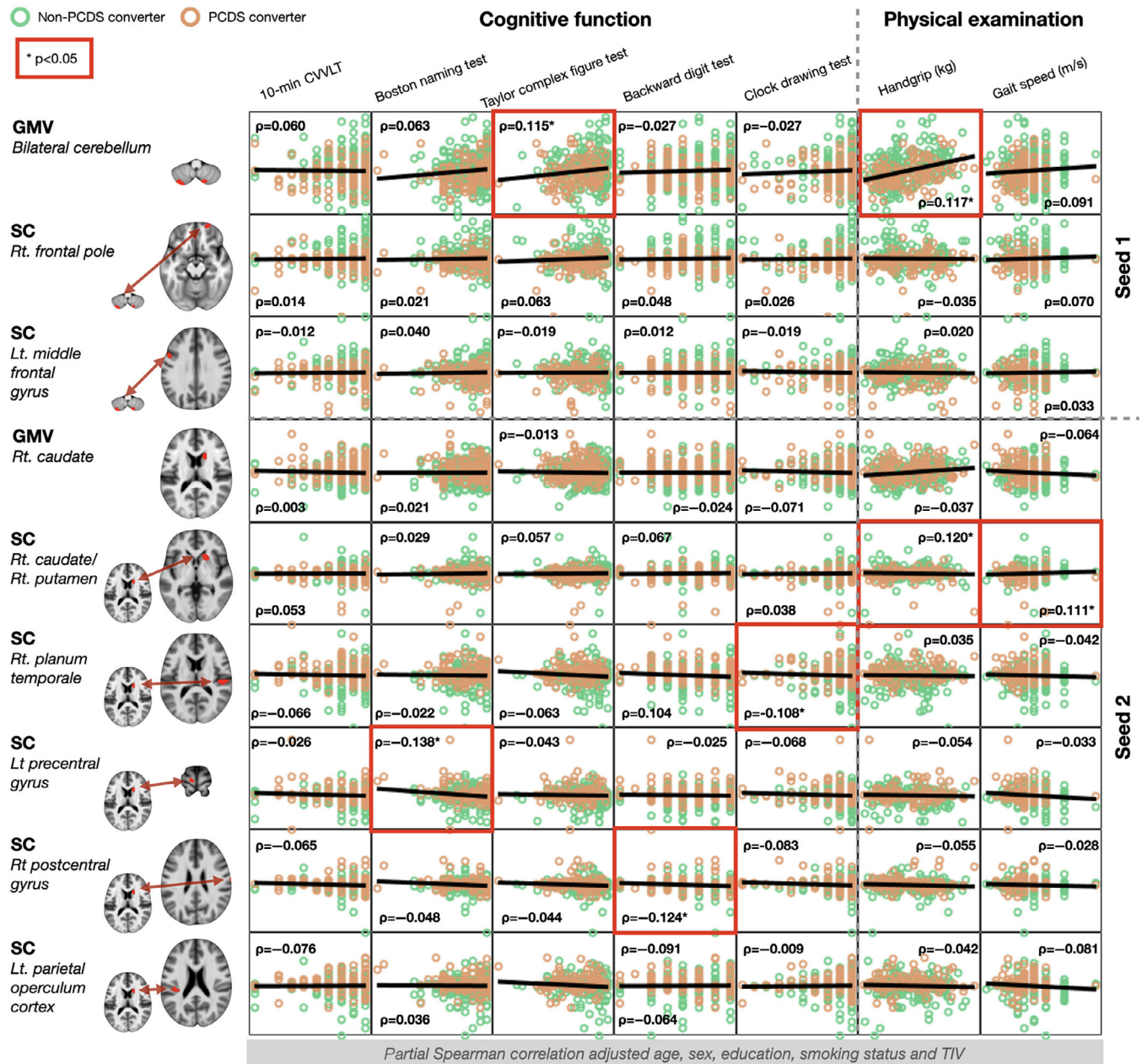


**FIGURE 4** Associations between identified neuroanatomic abnormalities including regional GMV and morphological network integrity and subsequent physical/cognitive functional performance. In validating the identified neuroanatomic correlates of PCDS, we expanded our investigation to examine the associations between these abnormalities and subsequent cognitive and mobility functions during follow-up. The results of partial Spearman correlation analyses adjusted for age, sex, education, smoking status, and total intracranial volume with an uncorrected  $p$  value  $< .05$  are marked with a red frame. The x-axis represents each neuroimaging measurement, while the y-axis represents cognitive or mobility functions. CVLT, Chinese version Verbal Learning Test; GMV, gray-matter volume; Lt., left; PCDS, physio-cognitive decline syndrome; Rt., right; SC, structural covariance; TIV, total intracranial volume.

thalamus, hippocampus, and cerebellum in PCDS individuals.<sup>11</sup> The present study establishes a temporal connection between neuroanatomical issues and PCDS using longitudinal analysis. We utilized voxel-wise GMV analysis and established SCNs in whole-brain MRI scans, comparing initial neuroimaging data of community-based older individuals who either developed or remained free from PCDS over a 6-year period. Our results reaffirm the cerebellum's significance in PCDS, aligning with our prior cross-sectional findings.

### 4.3 | Longitudinal neuroimaging studies

A recent neuroimaging study longitudinally explored neuroanatomic changes in older adults with accelerated declines in both physical and cognitive functions. The study identified dual decliners (dual decline in memory and gait;  $n = 28$  for neuroimaging analysis) based on cut-off values for annualized gait speed and memory performance decline.<sup>34</sup> Baseline brain volume comparisons of chosen ROIs did not

exhibit significant differences between those with and without dual decline, possibly due to the limited sensitivity of predefined ROI measurements compared to whole-brain voxel-wise analyses used in the present study. However, longitudinal analyses revealed greater volume reduction in dual decliners' specific regions (eg, superior frontal gyrus, superior parietal lobe, precuneus, thalamus, and cerebellum). Notably, among these regions, the cerebellum exhibited the most substantial disparity in volume decline rates between the two groups. This discovery aligns with prior and current research, underlining the central role of the cerebellum in driving both physical-mobility and cognitive decline in older adults.

#### 4.4 | Decreased SC in cerebellum-based morphological networks preceding the development of dual cognitive and mobility impairments

Our prior cross-sectional neuroimaging work identified reduced cerebellar GMV and cerebellum-hippocampus connections via diffusion-tensor imaging (DTI) analyses in older individuals with PCDS.<sup>11</sup> In this study with longitudinal clinical assessments, we employed SCNs to explore the underlying brain morphological networks associated with the emergence of PCDS. Similar disruptions in neurodegenerative diseases have been observed in brain networks derived from different MRI modalities, such as GM-SCN and resting-state functional MRI.<sup>35</sup> SC is used to analyze similarities in GM between brain regions and can be used to study networks of the brain by assessing differences in covariation among different brain regions across a population.<sup>36</sup> Our results showed that around 6 years before PCDS conversion, the cerebellum displayed decreased SC with the right frontal pole and left middle frontal gyrus in PCDS converters. Building on these insights, this study not only reinforces the cerebellum's critical significance in the well-being of older people but also reveals, for the first time, the involvement of cerebellum-frontal morphological network in the early pathophysiology of mobility frailty-related cognitive impairment. Our hypothesis posits that the cerebellum may be the foremost vulnerable or initial affected area in mobility frailty-related cognitive decline. This influence could potentially extend to its interconnected frontal regions, offering a potential explanation for the documented decrease in frontal GMV noted in earlier studies investigating concurrent declines in both mobility and cognitive functions.<sup>32,33</sup>

#### 4.5 | Alterations of caudate GMV and morphological networks preceding the development of dual cognitive and mobility impairments

Limited research has examined the caudate's GMV changes during aging. While declining caudate GMV is typically linked to reduced cognitive and motor functions,<sup>37,38</sup> our study yielded unexpected results. Our investigation found increased caudate GMV and enhanced connectivity to cerebral cortical regions among PCDS converters, contradicting prior expectations. This newfound observation might signify

a unique neuroanatomical trait associated with accelerated physical-mobility and cognitive aging. Understanding whether this change is detrimental or serves a compensatory role in PCDS requires further detailed exploration of its mechanisms.

#### 4.6 | Identifying clinical features linked to PCDS conversion

In this study, individuals who transitioned to PCDS were notably more inclined to be male and cigarette smokers compared to those who did not convert. A considerable and statistically significant sex difference was observed between nonconverters and converters (43.2% vs 62.1%,  $p = .001$ ), aligning with findings from our prior observational research examining PCDS progression in a community-based cohort.<sup>39</sup> In that study, which investigated potential risk factors for incident PCDS among robust participants, male sex emerged as a significant predictor for conversion. This sex-specific risk appears to be a distinct clinical feature associated with PCDS.

#### 4.7 | Study limitations & strength

This study is subject to certain limitations. The global consensus on defining dual cognitive and mobility impairments varies. A recent collaborative effort, spearheaded by the National Institute on Aging (NIA), has underscored the necessity for a unified operational definition encompassing terms such as "MCR," "PCDS," and "dual decline in memory and gait" to facilitate progress in this field.<sup>14</sup> Notably, PCDS has been rigorously characterized and validated as a clinical phenotype within a substantial Asian population, characterized by well-defined epidemiology, clinical trajectories, and outcomes.<sup>3,7-11,39,40</sup> Going forward, our focus will center on the application of PCDS criteria and/or the establishment of its substrate in more extensive and diverse cohorts. Furthermore, it should be noted that our study exclusively encompassed participants who underwent follow-up, revealing a cohort that skews toward youth, higher education levels, reduced vascular risk factors, and superior baseline verbal memory performance in comparison to those not included in the follow-up. Consequently, our findings are more relevant to a healthier subset of community-dwelling older individuals. Lastly, the interval between initial and final assessments ranged from 3 to 8 years. Acknowledging this limitation, we recognize that the actual conversion to the PCDS phenotype could have occurred at any point within this timeframe. Individuals not fully converting to PCDS at the final assessment may have been excluded, reflecting a challenge inherent in cohort studies with limited assessment time points. Future investigations will incorporate additional assessment time points to address this temporal consideration more comprehensively.

This study demonstrates multiple strengths. The ILAS population includes well-characterized community dwellers with thorough prospective assessments of physical mobility and cognitive abilities. We utilized voxel-based whole-brain analysis to detect

changes in regional GMV among PCDS converters. Unlike traditional morphometry, which outlines brain volume in specific ROIs, our approach avoids bias and potential oversight of smaller volume differences.

## 5 | CONCLUSION

The emerging preclinical dementia syndrome, characterized by combined accelerated physical mobility and cognitive decline, is evident in both Western and Asian populations, showing a specific pathophysiology based on initial evidence. This study's longitudinal approach has unveiled neuroanatomic alterations preceding the development of this syndrome in community-dwelling older individuals with intact cognitive and mobility functions. Echoing prior cross-sectional findings, our investigation highlights the cerebellum as a pivotal region linked to this syndrome. These results offer potential insights into early brain mechanisms driving dual cognitive and mobility impairments, potentially paving the way for a neuroanatomic biosignature, targeted treatments, and further exploration.

## ACKNOWLEDGMENTS

The authors would like to thank the Interdisciplinary Research Center for Healthy Longevity of National Yang Ming Chiao Tung University from the Featured Areas Research Center Program within the framework of the Higher Education Sprout Project by the Ministry of Education (MOE) in Taiwan for supporting the research work. This study was supported by the Center for Healthy Longevity and Aging Sciences, National Yang Ming University, Taipei, Taiwan; Center for Geriatrics and Gerontology, Taipei Veterans General Hospital, Taipei, Taiwan; and the Ministry of Science and Technology, Taiwan (NSTC 112-2321-B-075-004, NSTC 112-2321-B-A49-008, 111VACS-001, YSVH11002).

## CONFLICT OF INTEREST STATEMENT

No authors have conflicts of interest regarding this work. Author disclosures are available in the [supporting information](#).

## CONSENT STATEMENT

We conducted this observational cohort study following the Strengthening the Reporting of Observational Studies in Epidemiology (STROBE) guidelines. All participants provided written informed consent after thorough explanation by research nurses. The study protocol received approval from the institutional review boards of National Yang Ming University (YM103008) and Taipei Veterans General Hospital (2018-05-003B). The study adhered to the principles outlined in the Declaration of Helsinki in terms of its design and execution.

## ORCID

Chih-Kuang Liang  <https://orcid.org/0000-0003-1604-1600>

Chih-Ping Chung  <https://orcid.org/0000-0001-9419-9070>

## REFERENCES

- Hedden T, Gabrieli JD. Insights into the ageing mind: a view from cognitive neuroscience. *Nat Rev Neurosci*. 2004;5:87-96.
- Panza F, Lozupone M, Solfrizzi V, et al. Different cognitive frailty models and health- and cognitive-related outcomes in older age: from epidemiology to prevention. *J Alzheimers Dis*. 2018;62:993-1012.
- Chung CP, Lee WJ, Peng LN, et al. Physio-Cognitive decline syndrome as the phenotype and treatment target of unhealthy aging. *J Nutr Health Aging*. 2021;25:1179-1189.
- Panza F, Solfrizzi V, Barulli MR, et al. Cognitive frailty: a systematic review of epidemiological and neurobiological evidence of an age-related clinical condition. *Rejuvenation Res*. 2015;18:389-412.
- Kojima G, Taniguchi Y, Iliffe S, Walters K. Frailty as a predictor of Alzheimer disease, vascular dementia, and all dementia among community-dwelling older people: a systematic review and meta-analysis. *J Am Med Dir Assoc*. 2016;17:881-888.
- Chen LK, Woo J, Assantachai P, Auyeung TW, et al. Asian Working Group for Sarcopenia: 2019 consensus update on sarcopenia diagnosis and treatment. *J Am Med Dir Assoc*. 2020;21:300-307. e2.
- Lee WJ, Peng LN, Liang CK, Loh CH, Chen LK. Cognitive frailty predicting all-cause mortality among community-living older adults in Taiwan: a 4-year nationwide population-based cohort study. *PLoS One*. 2018;13:e0200447.
- Liu LK, Chen CH, Lee WJ, et al. Cognitive frailty and its association with all-cause mortality among community-dwelling older adults in Taiwan: results from I-Lan Longitudinal Aging Study. *Rejuvenation Res*. 2018;21:510-517.
- Shimada H, Makizako H, Doi T, et al. Combined prevalence of frailty and mild cognitive impairment in a population of elderly Japanese people. *J Am Med Dir Assoc*. 2013;14:518-524.
- Merchant RA, Chan YH, Hui RJY, et al. Motoric cognitive risk syndrome, physio-cognitive decline syndrome, cognitive frailty and reversibility with dual-task exercise. *Exp Gerontol*. 2021;150:111362.
- Liu LK, Chou KH, Hsu CH, et al. Cerebellar-limbic neurocircuit is the novel biosignature of physio-cognitive decline syndrome. *Aging (Albany NY)*. 2020;12:25319-25336.
- Vemuri P. Role of structural MRI in Alzheimer's disease. *Alzheimers Res Ther*. 2010;2:23.
- Chen WT, Chou KH, Liu LK, et al. Reduced cerebellar gray matter is a neural signature of physical frailty. *Hum Brain Mapp*. 2015;36:3666-3676.
- Tian Q, Montero-Odasso M, Buchman AS, et al. Dual cognitive and mobility impairments and future dementia—Setting a research agenda. *Alzheimers Dement*. 2023;19:1579-1586.
- Verghese J, Ayers E, Barzilai N, et al. Motoric cognitive risk syndrome: multicenter incidence study. *Neurology*. 2014;83:2278-2284.
- Ashburner J, Friston KJ. Voxel-based morphometry—the methods. *Neuroimage*. 2000;11:805-821.
- Ashburner J. A fast diffeomorphic image registration algorithm. *Neuroimage*. 2007;38:95-113.
- Gaser C, Dahnke R, Thompson PM, Kurth F, Luders E. CAT—a computational anatomy toolbox for the analysis of structural MRI data. *BioRxiv*. 2022.
- Bernhardt BC, Worsley KJ, Besson P, et al. Mapping limbic network organization in temporal lobe epilepsy using morphometric correlations: insights on the relation between mesiotemporal connectivity and cortical atrophy. *Neuroimage*. 2008;42:515-524.
- Saggar M, Hosseini SM, Bruno JL, et al. Estimating individual contribution from group-based structural correlation networks. *Neuroimage*. 2015;120:274-284.
- Liu Z, Palaniyappan L, Wu X, et al. Resolving heterogeneity in schizophrenia through a novel systems approach to brain structure: individualized structural covariance network analysis. *Mol Psychiatry*. 2021;26:7719-7731.

22. Schmahmann JD, Guell X, Stoodley CJ, Halko MA. The theory and neuroscience of cerebellar cognition. *Annu Rev Neurosci*. 2019;42:337-364.
23. Arleo A, Bareš M, Bernard JA, et al. Consensus paper: cerebellum and ageing. *Cerebellum*. 2023. Jul 10 (ePub ahead of print).
24. Habas C. Functional connectivity of the cognitive cerebellum. *Front Syst Neurosci*. 2021;15:642225.
25. Habas C, Manto M, Cabaraux P. The cerebellar thalamus. *Cerebellum*. 2019;18:635-648.
26. Krienen FM, Buckner RL. Segregated fronto-cerebellar circuits revealed by intrinsic functional connectivity. *Cereb Cortex*. 2009;19:2485-2497.
27. Brissenden JA, Levin EJ, Osher DE, Halko MA, Somers DC. Functional evidence for a cerebellar node of the Dorsal Attention Network. *J Neurosci*. 2016;36:6083-6096.
28. Fried LP, Tangen CM, Walston J, et al. Frailty in older adults: evidence for a phenotype. *J Gerontol A Biol Sci Med Sci*. 2001;56:M146-156.
29. Petermann-Rocha F, Lyall DM, Gray SR, et al. Associations between physical frailty and dementia incidence: a prospective study from UK Biobank. *Lancet Healthy Longev*. 2020;1:e58-e68.
30. Wu YH, Liu LK, Chen WT, et al. Cognitive Function in individuals with physical frailty but without dementia or cognitive complaints: results from the I-Lan Longitudinal Aging Study. *J Am Med Dir Assoc*. 2015;16:899. e9-16.
31. Jiang R, Noble S, Sui J, et al. Associations of physical frailty with health outcomes and brain structure in 483 033 middle-aged and older adults: a population-based study from the UK Biobank. *Lancet Digit Health*. 2023;5:e350-e359.
32. Beauchet O, Allali G, Annweiler C, Verghese J. Association of motoric cognitive risk syndrome with brain volumes: results from the GAIT study. *J Gerontol A Biol Sci Med Sci*. 2016;71:1081-1088.
33. Blumen HM, Allali G, Beauchet O, Lipton RB, Verghese J. A gray matter volume covariance network associated with the motoric cognitive risk syndrome: a multicohort MRI study. *J Gerontol A Biol Sci Med Sci*. 2019;74:884-889.
34. Tian Q, Studenski SA, Montero-Odasso M, Davatzikos C, Resnick SM, Ferrucci L. Cognitive and neuroimaging profiles of older adults with dual decline in memory and gait speed. *Neurobiol Aging*. 2021;97:49-55.
35. Alexander-Bloch A, Giedd JN, Bullmore E. Imaging structural co-variance between human brain regions. *Nat Rev Neurosci*. 2013;14:322-336.
36. Mechelli A, Friston KJ, Frackowiak RS, Price CJ. Structural covariance in the human cortex. *J Neurosci*. 2005;25:8303-8310.
37. Macpherson T, Hikida T. Role of basal ganglia neurocircuitry in the pathology of psychiatric disorders. *Psychiatry Clin Neurosci*. 2019;73:289-301.
38. Alexander GE, Crutcher MD. Functional architecture of basal ganglia circuits: neural substrates of parallel processing. *Trends Neurosci*. 1990;13:266-271.
39. Lee WJ, Peng LN, Lin MH, et al. Six-year transition of physio-cognitive decline syndrome: results from I-Lan Longitudinal Aging Study. *Arch Gerontol Geriatr*. 2022;102:104743.
40. Lin YC, Chung CP, Lee PL, et al. The flexibility of physio-cognitive decline syndrome: a Longitudinal Cohort Study. *Front Public Health*. 2022;10:820383.

### SUPPORTING INFORMATION

Additional supporting information can be found online in the Supporting Information section at the end of this article.

**How to cite this article:** Lee PL, Chou KH, Lee WJ, et al. Altered cerebellar and caudate gray-matter volumes and structural covariance networks preceding dual cognitive and mobility impairments in older people. *Alzheimer's Dement*. 2024;20:2420-2433. <https://doi.org/10.1002/alz.13714>